Chapter 1. Introduction

In geophysics there is increasing interest in modeling spatially nonuniform stress, i.e., spatially heterogeneous stress, on 2D planar faults as a means of explaining a variety of geophysical phenomena. This thesis goes beyond 2D and models the effect of 3D spatially heterogeneous stress on focal mechanism orientations, seismic clustering, stress rotations after mainshocks, and strength of the crust. We ask, what happens when one drops the assumption that stress is approximately spatially uniform in the crust. We find that there is ample reason to believe that stress is spatially heterogeneous in 3D for some regions (Figures 1.1–1.3), and including heterogeneity may profoundly change how one interprets seismic observables. It is our hope that by modeling stress heterogeneity statistically, we can encourage others to view stress in the crust from a substantially different perspective. The problems addressed in this thesis using heterogeneous stress are only the tip of the iceberg for what we hope will be a rich research field in the future.

Observations of Heterogeneous Stress

Observations of spatially varying slip along fault zones and in earthquakes suggest that both slip and stress are very spatially heterogeneous and possibly fractal in nature [*Andrews*, 1980; 1981; *Ben-Zion and Sammis*, 2003; *Herrero and Bernard*, 1994; *Lavallee and Archuleta*, 2003; *Mai and Beroza*, 2002; *Manighetti, et al.*, 2005; *Manighetti, et al.*, 2001]. For example, McGill and Rubin [1999] observed a 1 m change in slip over a distance of approximately 1 km in the Landers earthquake, which is a 10^{-3} strain change. This implies possibly a 100 MPa stress change over the distance of 1 km. The observed strain and stress change reported by McGill and Rubin is just one example

indicating the Earth may contain large stress fluctuations over small spatial wavelengths. Similar strain changes can be seen in the slip inversion from the Landers earthquake [*Wald and Heaton*, 1994] (Figure 1.1). Another example of highly variable, heterogeneous slip over short wavelengths comes from Manighetti et al. [2001] (Figure 1.2). Using altimetry data in the Afar depression, East African rift, they show heterogeneous cumulative slip as a function of distance, with short wavelength strains of the order $5x10^{-2}$. While it is true that non-elastic processes may come into play at such large shear strains, it does demonstrate a few features. Heterogeneous slip patterns exist not just for individual earthquake slip histories but persist for the entire cumulative slip history of fault zones, indicating that slip heterogeneity is a stable feature. In addition, the cumulative slip shows possibly self-similar, fractal patterns as seen in Figure 1.2b; i.e., subsections of cumulative slip have similar slip heterogeneity patterns as the sum of all the subsections.

Borehole studies, which measure the orientation of maximum horizontal compressive stress directly from borehole breakouts, also indicate that stress can be quite heterogeneous. Figure 1.3, a summary figure from Wilde and Stock [1997], shows the inferred directions of S_H, the maximum horizontal compressive stress, from borehole breakouts. Multiple boreholes with different orientations had been drilled at approximately the same locations, which Wilde and Stock analyzed to constrain the relative magnitudes of the principal stresses. What is most interesting to our study is that boreholes drilled within close proximity of each other can show greatly varying S_H orientations, indicative of heterogeneous stress (Figure 1.3). Figure 1.4, taken from a

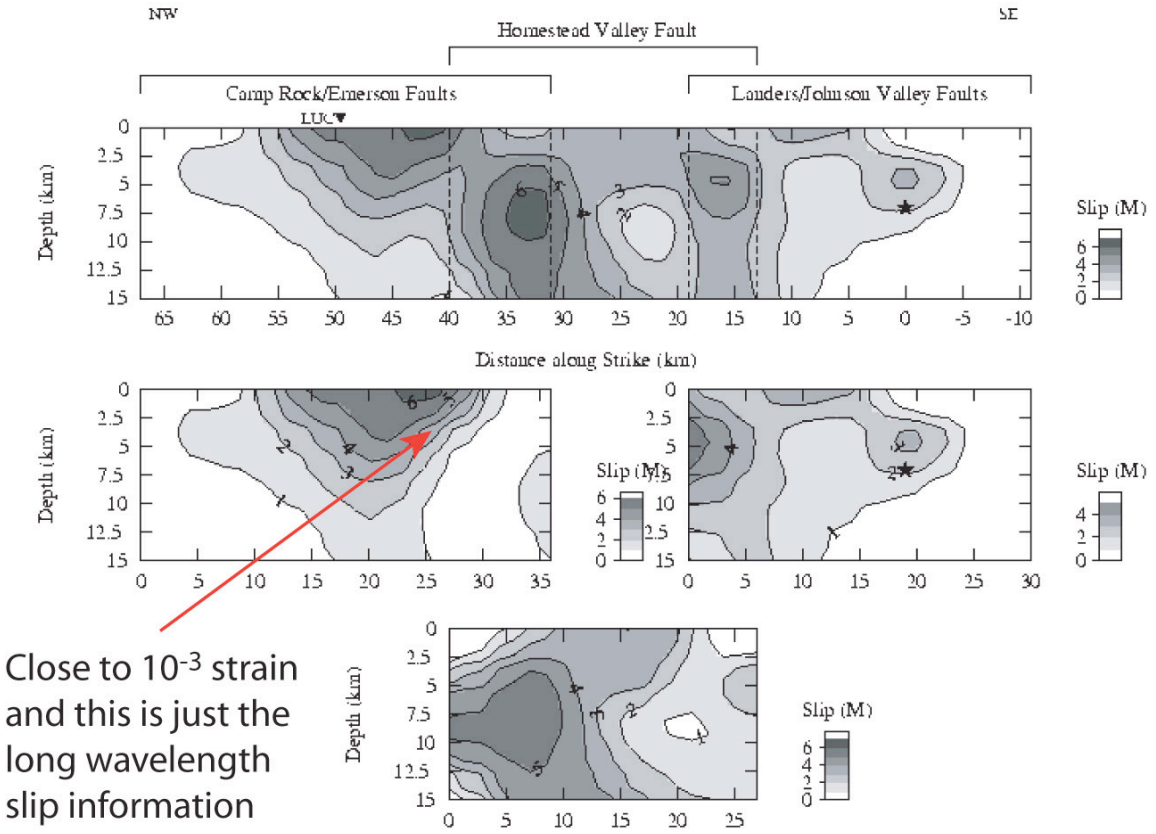

Figure 1.1. *Figure modified from Wald and Heaton [Wald and Heaton, 1994] showing the final slip distribution for the 1992 Landers earthquake. The contours are for 1m slip intervals with the higher slips shaded with darker greys. There are places within the slip distribution on this figure where the strain is approximately* 10^{-3}. *The strain varies over the surface of the rupture, which would produce stress changes over the surface of the rupture and lock in heterogeneous stress. This slip distribution is limited by the data to longer wavelength variations in slip; therefore, there may be even shorter wavelength spatial stress heterogeneity that was locked in by the dynamic rupture process.*

study of the Cajon pass borehole [*Barton and Zoback*, 1994], also shows significant heterogeneity in the orientations of borehole breakouts for an individual borehole near an active fault. The + signs or pulses represent the actual breakout data from the Cajon well, and the triangles represent the modeled breakouts from Barton and Zoback [1994]. There are variations in the breakout orientations over different lengthscales, and there is an anomaly at approximately 2850 m depth, but the feature we find most interesting is the short length-scale variations in the orientations of S_H. In places there is an approximately 90° rotation of S_H over a 1–10 m length. This would appear to support our hypothesis that stress can be quite heterogeneous over short length-scales in tectonically active regions.

Liu-Zeng et al. [2005] have also shown that the assumption of short wavelength heterogeneous fractal slip can reproduce distributions of earthquakes having slip vs. length ratios similar to real earthquakes and realistic Gutenberg-Richter frequency magnitude statistics. Using simple stochastic models, they showed that spatially connected slip can produce averaged stress drops (a constant times average slip divided by rupture length) similar to real data.

Perhaps the most interesting piece of data comes from Zoback and Beroza [1993] (Figure 1.5). They studied the orientations of aftershock planes from the Loma Prieta earthquake and plotted their distributions as a function of strike and dip. Interestingly, they found aftershocks that had both right-lateral and left-lateral orientations on similar fault planes as well as normal and reverse orientations. Given that this is considered a San Andreas fault earthquake and the San Andreas fault is a strongly right-lateral fault, the existence of left-lateral aftershocks on fault planes parallel to the San Andreas Fault

presents a curious problem. Zoback and Beroza proposed that the principal compressive stress direction was almost normal to the fault and that the aftershocks occurred on extremely weak faults of different orientations surrounding the mainshock zone. However, if one allows for the new paradigm of spatially heterogeneous stress in three dimensions, which is being advocated in this thesis, the left-lateral orientations naturally occur. Figure 1.6, taken from Chapter 5, shows our initial hypothesis for what a 1D cross section of shear stress in Northern or Southern California might look like. While most of the points have positive shear stress on the σ_{12} plane, a small percentage have negative shear stress on the σ_{12} plane. Heterogeneity similar to this could explain why Zoback and Beroza observed left-lateral aftershocks after the Loma Prieta earthquake; the large local stress change to the system from the mainshock, combined with stress heterogeneity in the left-lateral direction, would create the left-lateral aftershocks.

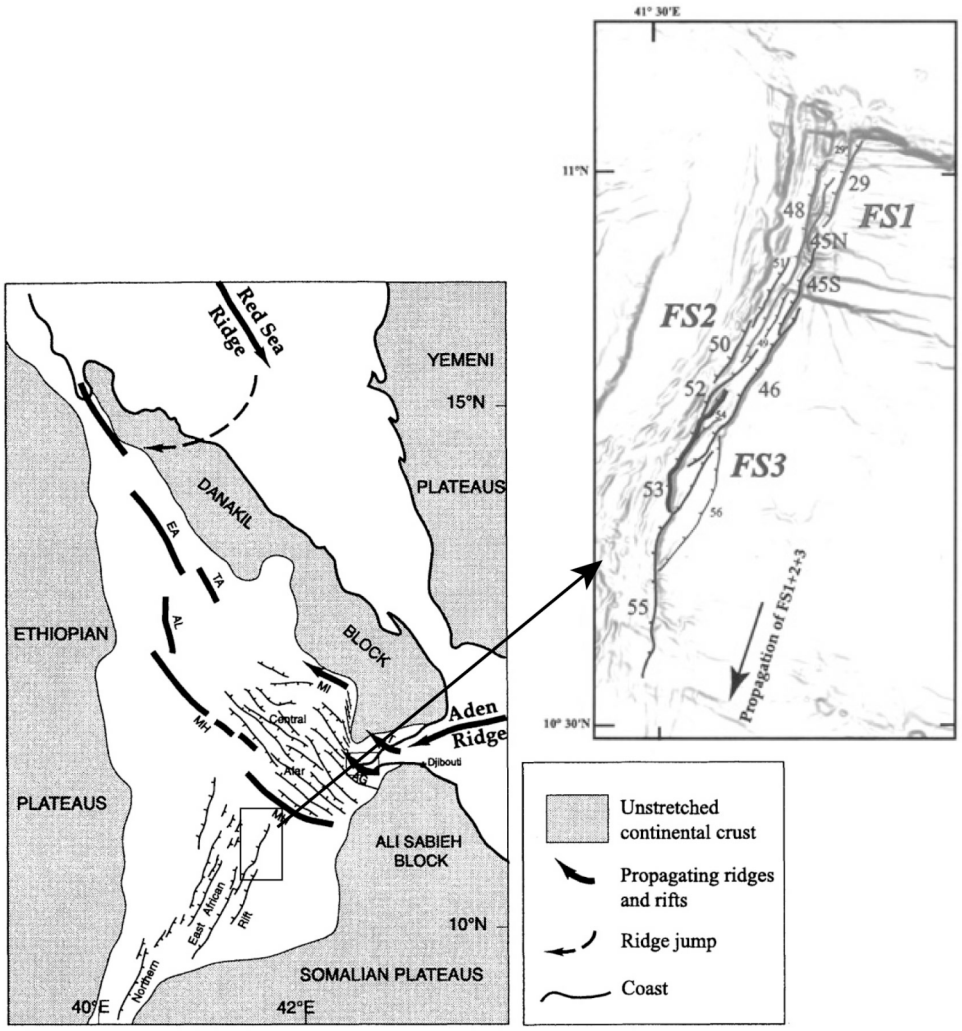

Figure 1.2 a)

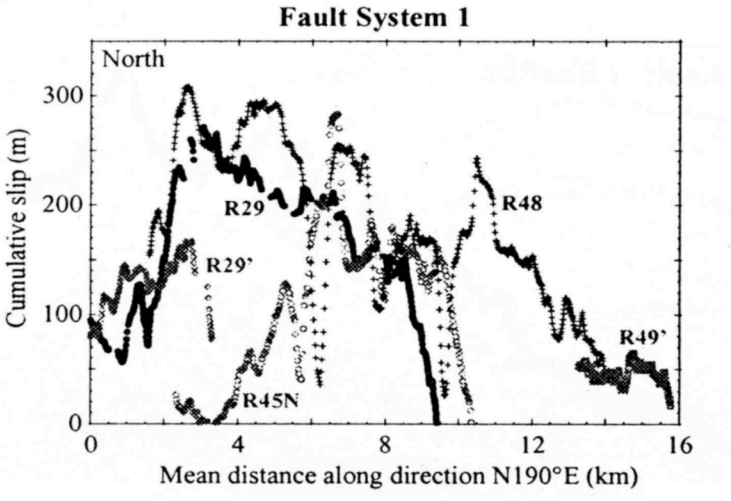

Figure 1.2 b)

Figure 1.2. *Sample evidence of large stress and strain spatial heterogeneity due to a series of earthquakes (from Manighetti et al., 2001).* ***a)*** *A map of the fault system 1, in the East African Rift.* ***b)*** *Typical slip vs. length plots within one of the fault systems. There is great spatial heterogeneity in slip, which implies short wavelength strains of the order* $5x10^{-2}$.

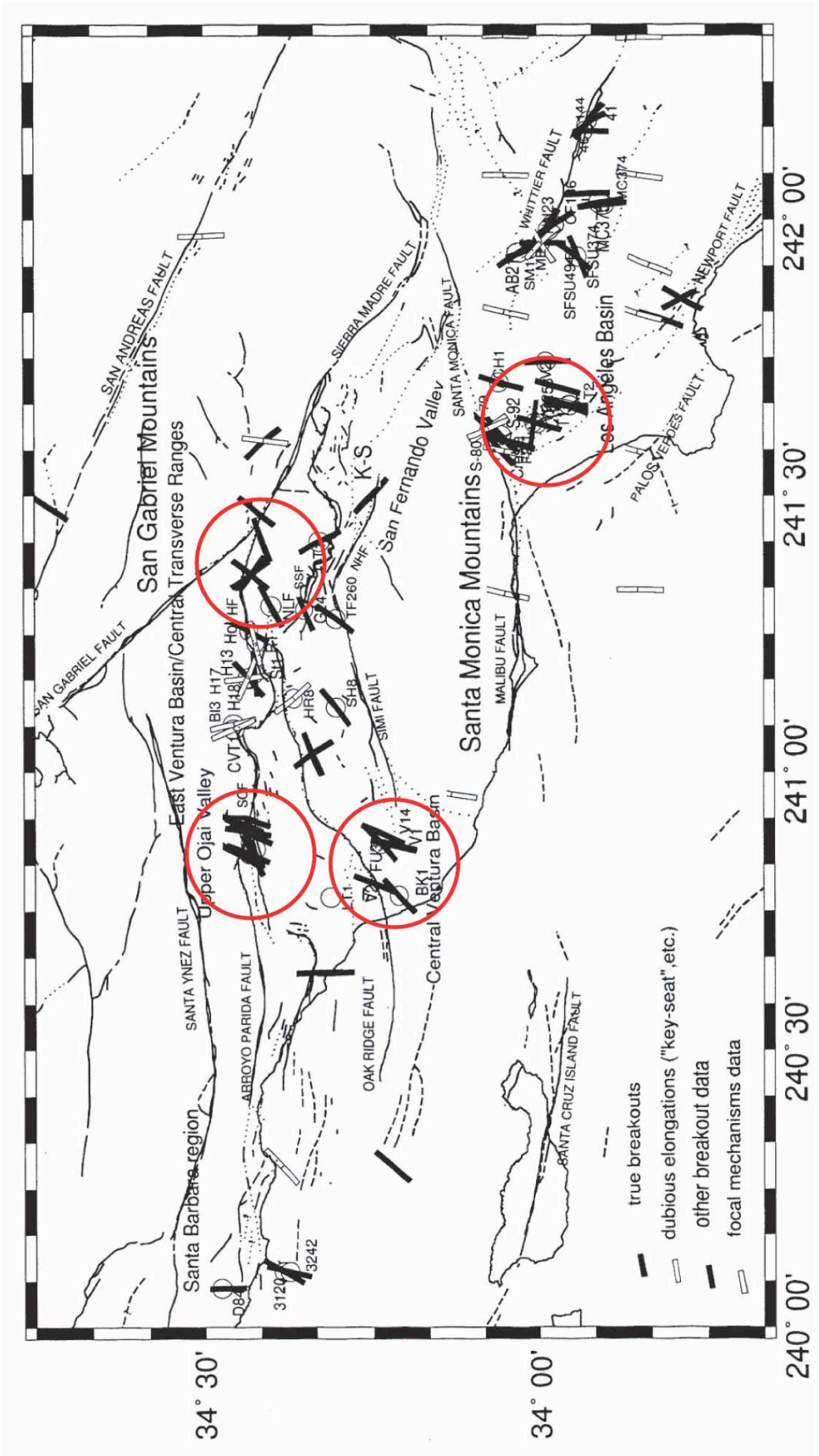
SAN ANDREAS FAULT
San Gabriel Mountains
East Ventura Basin/Central Transverse Ranges
SIERRA MADRE FAULT
SAN GABRIEL FAULT
San Fernando Valley
SANTA MONICA FAULT
Santa Monica Mountains
Los Angeles Basin
WHITTIER FAULT
NEWPORT FAULT
PALOS VERDES FAULT
Upper Ojai Valley
SANTA YNEZ FAULT
ABROYO PARIDA FAULT
OAK RIDGE FAULT
SIMI FAULT
MALIBU FAULT
Central Ventura Basin
Santa Barbara region
SANTA CRUZ ISLAND FAULT
true breakouts
dubious elongations ("key-seat",etc.)
other breakout data
focal mechanisms data
34° 30'
34° 00'
240° 00'
240° 30'
241° 00'
241° 30'
242° 00'

Figure 1.3. *Wilde and Stock [1997] plotted inferred maximum horizontal compressive stress, S_H, orientations from borehole breakouts in Southern California. There are a variety of orientations for borehole breakouts from the same borehole or from boreholes spatially close to one another. This suggests short-wavelength spatial stress heterogeneity. In this modified plot, we have used red circles to point out a few of the locations studied by Wilde and Stock that show evidence for S_H orientation heterogeneity.*

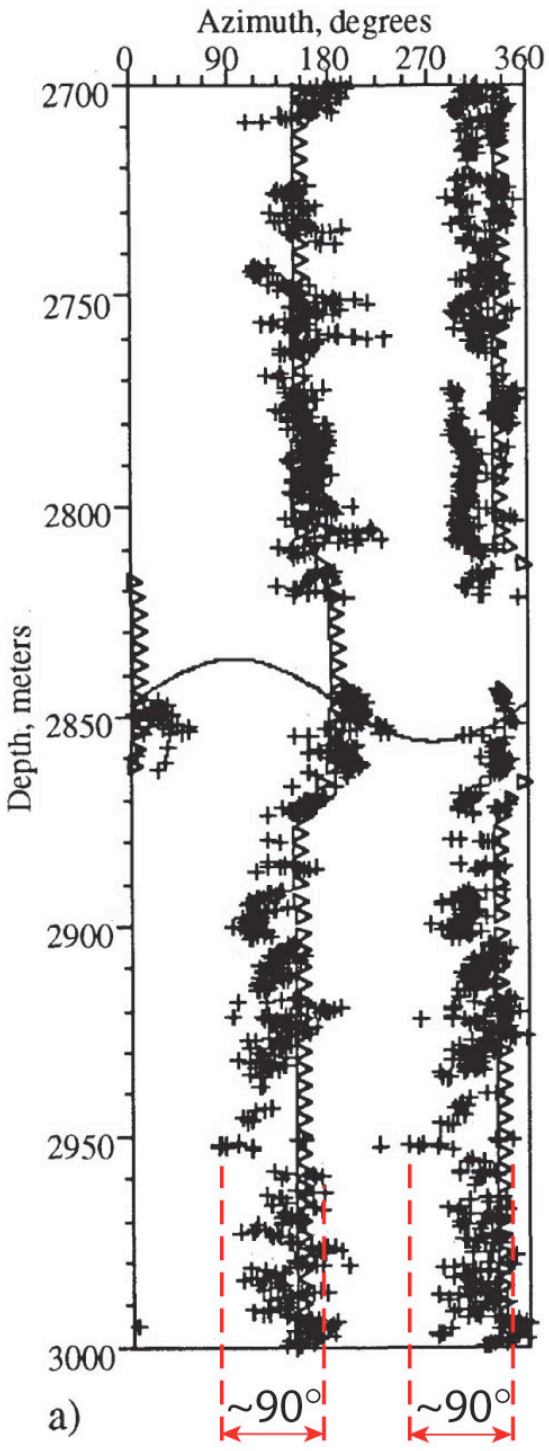

Example of an Approximately 90° Rotation of the Maximum Horizontal Compressive Stress over a Distance of 1–10 m

Figure 1.4. *Barton and Zoback [1994] plotted maximum horizontal compressive stress, S_H, azimuth as a function of depth for breakouts in the Cajon Pass borehole. The plus signs are the breakout data and the triangles represent Barton and Zoback's model. There is an anomaly at 2850 m depth, and there is significant short wavelength rotation of S_H as a function of depth. In this modified figure, we have shown a sample location with an approximately 90° rotation of S_H over a distance of 1–10 m. This provides support for our hypothesis that there can be significant short wavelength stress heterogeneity in tectonically active regions.*

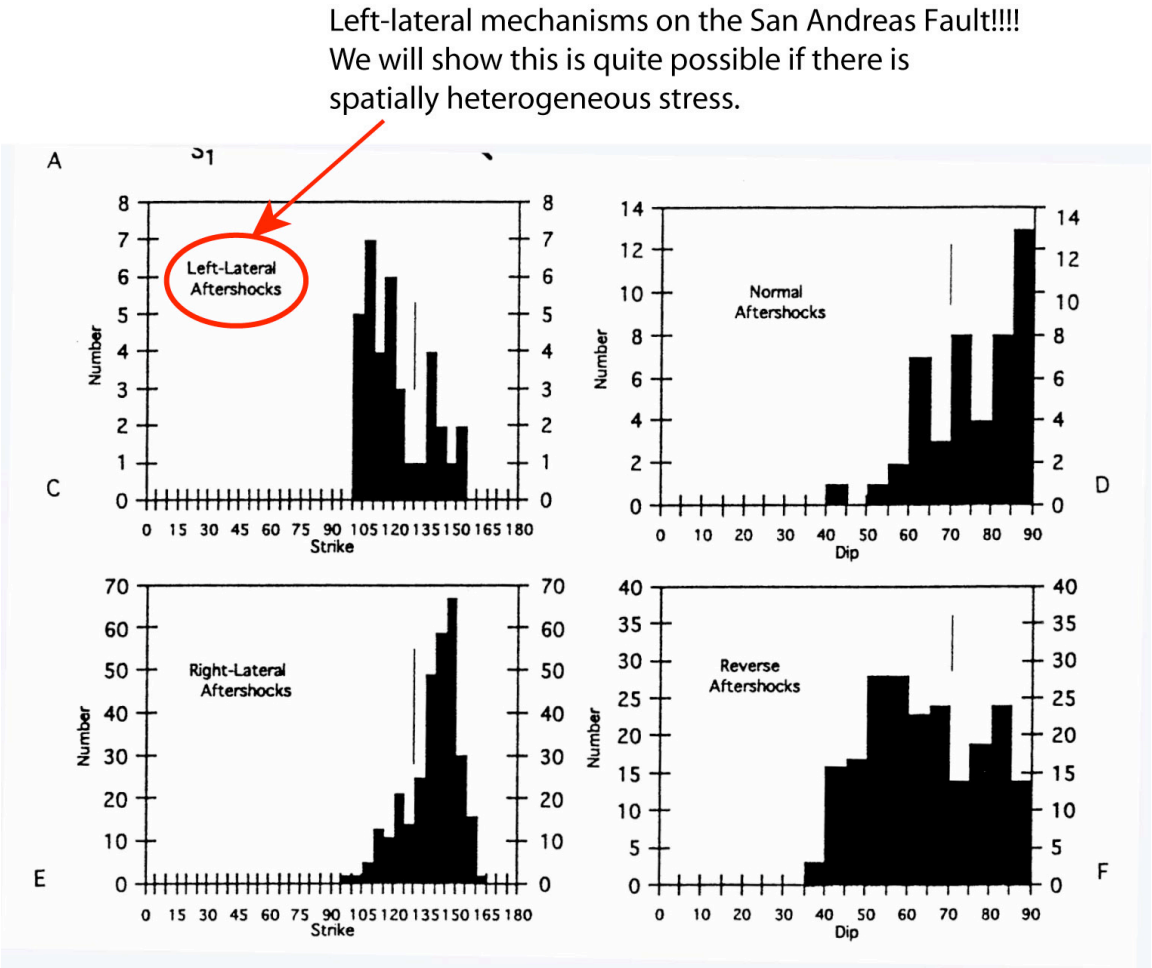

Figure 1.5. *Figure modified from Zoback and Beroza [1993] shows histograms of the different aftershock orientations. Most of the aftershocks had a right-lateral fault orientation. About 10% had left-lateral orientation. We propose that stress heterogeneity is the most natural explanation for left-lateral mechanisms on the right-lateral San Andreas Fault.*

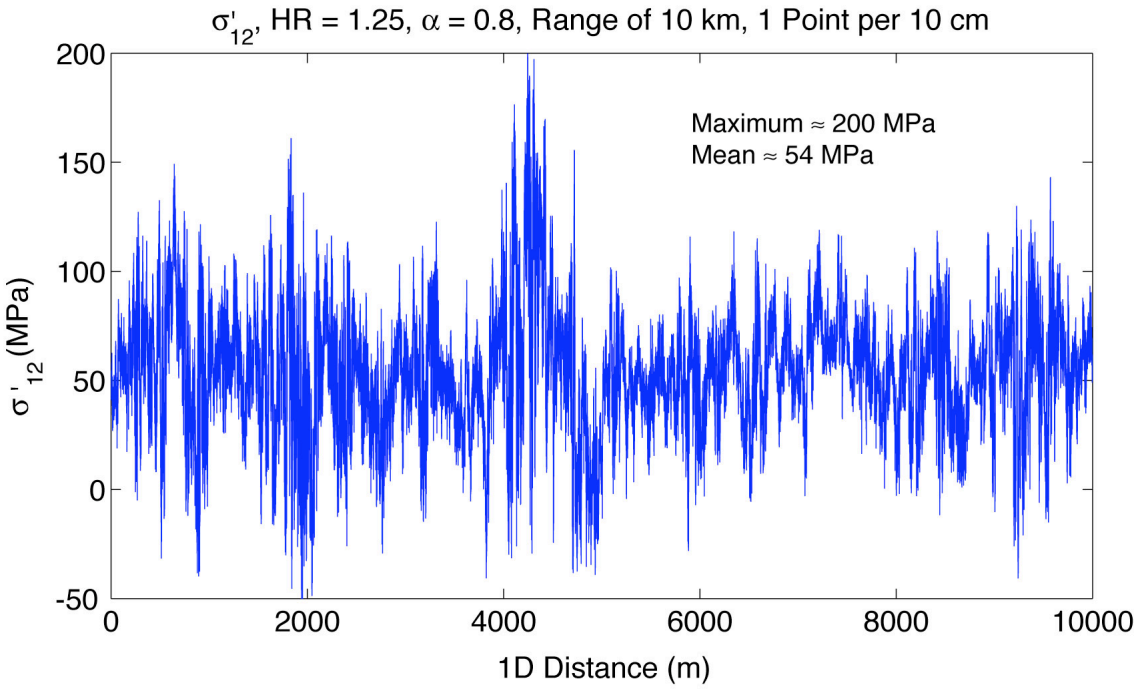

Figure 1.6. *Figure taken from Chapter 5 of this thesis. If the spatial stress heterogeneity has a moderate to large amplitude compared to the spatial mean stress, there will exist both points with positive shear stress and points with negative shear stress. Therefore, it is possible in a right-lateral shear stress regime to have a few left-lateral aftershocks as seen in Figure 1.5.*

Motivation for Heterogeneous Stress from Dynamics Ruptures

Now that we know fractal-like, spatially heterogeneous slip and heterogeneous stress is observed in the real Earth and that heterogeneous slip/stress is compatible with seismic observables, one may ask, how does the Earth possibly produce this spatial heterogeneity.

In the dynamic paradigm, we find that simulated dynamic earthquake ruptures produce increasingly heterogeneous slip as the dynamic friction becomes increasingly sensitive to the slip velocity. This is what Aagaard and Heaton [in preparation, 2006] discovered when they simulated long earthquake sequences on a planar fault subject to constant shear strain in time. If the value of dynamic friction in the real Earth is quite sensitive to changes in the slip velocity, it could explain observed slip heterogeneity; and indeed, there is evidence this may be true. The argument is as follows. Exhumed faults tend to yield thin primary deformation zones indicating there is little to no melting during the dynamic earthquake rupture [*Sibson*, 2003]. Given the typical sliding velocities of 1 m/s, it suggests that the dynamic friction value is quite small for the duration of the rupture; otherwise, one would see significant pseudotachylyte friction-melt. Heat flow studies of the San Andreas Fault also yield anomalously low heat flow values for a dynamic coefficient of friction of $\mu \approx 0.6$ [*Lachenbruch and Sass*, 1980], again indicating that the dynamic coefficient of friction may be small. A possible explanation is that there is a sudden transition from the high static friction, $\mu > 0.6$, to low dynamic friction, $\mu < 0.1$, in the vicinity of the rupture front, with a similar transition back to high friction as one moves away from the rupture front, i.e., extreme velocity weakening. Interestingly, this is similar to Rice's [1999] flash heating friction law and experimental

results reported by Tullis and Goldsby [2005] where they observed dramatic reductions in sliding friction for velocities $> 50\ cm/s$, possibly flash heating. Tullis, in a recent presentation [*Tullis*, 2005] available online at http://online.itp.ucsb.edu/online/earthq05/tullis, showed plots of friction coefficient as a function of sliding velocity for three different materials: quartz, granite, and gabbro. The low velocity friction coefficients range from a little over 0.6 to approximately 0.9 depending on the material. At sliding velocities of $> 50\ cm/s$, the sliding coefficient of friction approaches a value of 0.2. Interestingly, these experiments also observe instantaneous full healing. This combination of high static friction, low sliding friction, and instantaneous healing back to high static friction will freeze in short length-scale stress heterogeneity, i.e., abrupt spatial stress changes along the length of the fault.

In flash heating, as the two sides of the fault begin sliding past some threshold velocity under normal stress and with asperities, a thin layer melts and dramatically lowers the coefficient of friction for a short time. After flash heating, other mechanisms may be activated such as full or partial melting and pore pressure evolution. If the real Earth experiences flash heating or other strongly velocity dependent effects during earthquakes, then it is quite plausible that very heterogeneous stresses would be locked into the crust when high dynamic stresses are frozen in by the sudden transitions from static to dynamic friction, then back to static friction. This is a length-scale independent effect. Since the two types of stress states that are compatible with length-scale independent processes are homogeneous stress and fractal stress, we believe some type of fractal heterogeneous stress is a good initial hypothesis.

Of interest, Rice, Lapusta and Ranjith [2001] showed through theoretical studies that there are problems with only velocity-dependent friction that have no solution (i.e., are ill-posed). The problems do not converge; i.e. there is no solution as you reduce the grid size. We hypothesize that a fractal heterogeneous solution (with no inherent length-scale) might be the answer to this problem.

A static effect that can also produce heterogeneous stress was recently presented by Dieterich [2005]. Fault traces in nature are rarely if ever completely planar; there is usually some small-scale 3D geometry to the fault trace. Modeling fault traces with fractal geometry, solving for slip with boundary elements and using a $\mu = 0.6$, he found that even very small variations in fault trace can produce significant near-fault stress heterogeneity and create spatially heterogeneous aftershock rates. In this case, the coefficient of friction was not varied dynamically, so this is an entirely independent effect that also creates stress heterogeneity.

Stress Model to Be Used in the Thesis

In this thesis, we create 3D grids like Figure 1.7, where the full or deviatoric stress tensor is defined at each spatial grid point using equation (1.1). The principal stresses and orientations of the heterogeneous stress tensor, $\boldsymbol{\sigma}'_H(\mathbf{x})$, are randomly generated; then a discrete spatial filter is applied to produce power-law spatial stress heterogeneity. Chapters 2 and 3 explain how we do this in detail. A spatially and temporally homogeneous stress tensor, $\boldsymbol{\sigma}'_B$, what stress inversions approximately solve for, is added. Last, points are brought to failure by adding on a linearly increasing tectonic stress due to the stress rate, $\dot{\boldsymbol{\sigma}}'_T$, and applying a plastic yield failure criterion.

This generates point failures within our 3D grid, which we call earthquakes, and produces our set of synthetic focal mechanisms. Chapter 4 shows the steps of bringing points to failure as well as simulations that demonstrate how large amplitude spatially heterogeneous stress biases stress inversions toward the stress rate tensor, $\dot{\boldsymbol{\sigma}}'_T$.

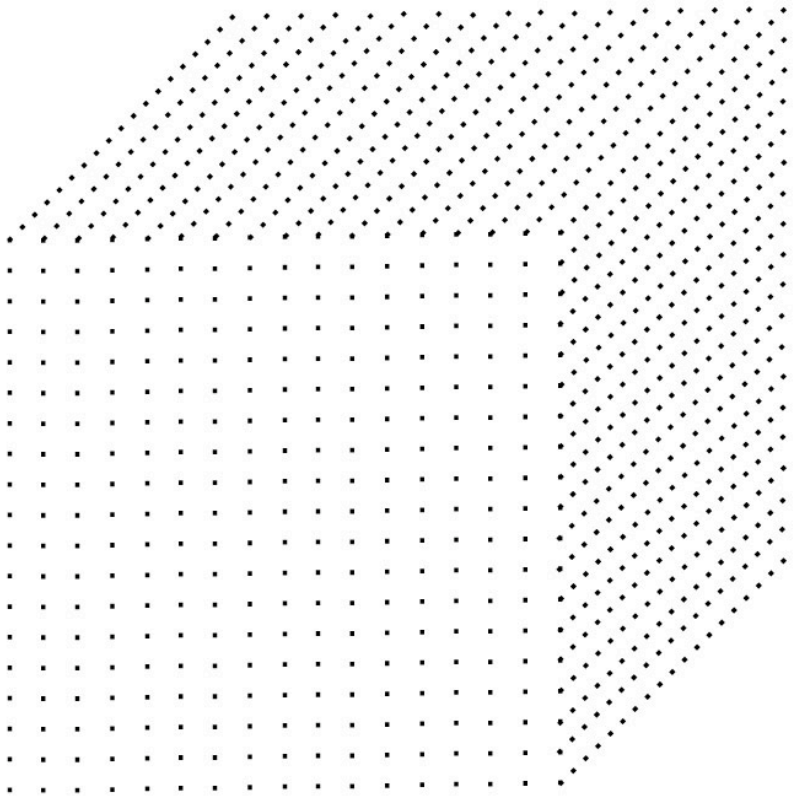

Figure 1.7. *A sample 3D grid of points. In our numerical simulations we would define the full or deviatoric stress tensor at each spatial grid point.*

In creating equation (1.1) we approximate stress in time and space as a decomposition that is a linear sum of parts that are 1) spatially and temporally uniform, 2) varying with time, but relatively homogeneous spatially, and 3) spatially very heterogeneous, but do not vary much over the time scale of decades. While there are many features of real mechanics that are not included in this description but are discussed more in the following section, this is the simplest decomposition that we could think of, which also contains the essential features of a temporally varying stochastic stress model.

$$\boldsymbol{\sigma}'(\mathbf{x},t) = \boldsymbol{\sigma}'_B + \dot{\boldsymbol{\sigma}}'_T t + \boldsymbol{\sigma}'_H(\mathbf{x}) \tag{1.1}$$

Where

$\boldsymbol{\sigma}'_B$ is the background stress, which is the spatially and temporally averaged stress tensor in the region of interest. This is the quantity that traditional stress inversions are designed to find.

$\dot{\boldsymbol{\sigma}}'_T(t)$ is the temporally varying stress due to plate tectonics. For example, if there is far-field loading but the fault in the brittle upper crust is locked, there can be a temporal increase of stress as a function of time (Figure 1.8). There may also be fault interactions that can produce regional stress rates similar to what is seen in Figure 1.9, modified from Becker et al. [2003] for Southern California. Or short-term stress rates could be created by post-seismic visco-elastic relaxation.

This term is assumed to grow linearly with time for our short simulation time windows of 10–20 years, but is assumed to be small compared to $\boldsymbol{\sigma}'_H(\mathbf{x})$ and $\boldsymbol{\sigma}'_B$. While, in reality, it varies with space, the spatial variations are small by St. Venant's principle since the forces are applied at a distance. In general, we

assume that $\boldsymbol{\sigma}'_B$ and $\dot{\boldsymbol{\sigma}}'_T$ have different orientations. For example, the principal compression of the average background stress might be oriented nearly perpendicular to the San Andreas Fault [*Townend and Zoback*, 2004]; whereas, the stress rate compression axis must be at a 45° angle, since shear on the San Andreas Fault accommodates most of the plate motion. Simulations in Chapter 4 explore this possibility.

$\boldsymbol{\sigma}'_H(\mathbf{x})$ is spatially varying stress. By definition, its spatial average is zero. The heterogeneous stress is assumed to be due to all of the stress changes caused by local inelastic deformations such as the slip distribution due to faulting, compaction, fluids, thermal stresses, topography, etc. The heterogeneity is described by two parameters,

1. α, where the amplitude spectrum of any 1D cross section through our 3D $\boldsymbol{\sigma}'_H(\mathbf{x})$ grid is proportional to $1/k^{\alpha}$ and [*Barnsely, et al.*, 1988]

2. ***Heterogeneity Ratio*** $= HR = \dfrac{\sqrt{Mean\left[Spatially\ Heterogeneous\ I'_2\right]}\ \left[\text{Units of Stress}\right]}{\sqrt{Spatially\ Uniform\ Background\ Stress\ I'_2}\ \left[\text{Units of Stress}\right]}$, which is a dimensionless number relating the size of the heterogeneity to the size of the background stress to create a dimensionless heterogeneity amplitude. I'_2, the second invariant of the deviatoric stress tensor, a nonnegative number, is a measure of maximum shear stress regardless of orientation, and is the quantity used in our primary failure criterion. That is why we use I'_2 for our measure of heterogeneity amplitude.

We also assume that the stochastic properties of $\boldsymbol{\sigma}'_H(\mathbf{x})$, described by *HR* and α, do not significantly evolve in time for the simulations we present in the thesis; therefore, we do not update $\boldsymbol{\sigma}'_H(\mathbf{x})$ after each event. Specifically, we are interested in stress inversions that are applied to background seismicity, in between major seismic events over a time window in the range of 1–20 years. A major event will significantly change the 3D stress pattern and would have to be taken into account, which is a future research direction we have begun delving into. However, we assume that the heterogeneous slip patterns, after some stress relaxation, regenerate heterogeneous stress that will have approximately the same stochastic properties as before the major earthquake.

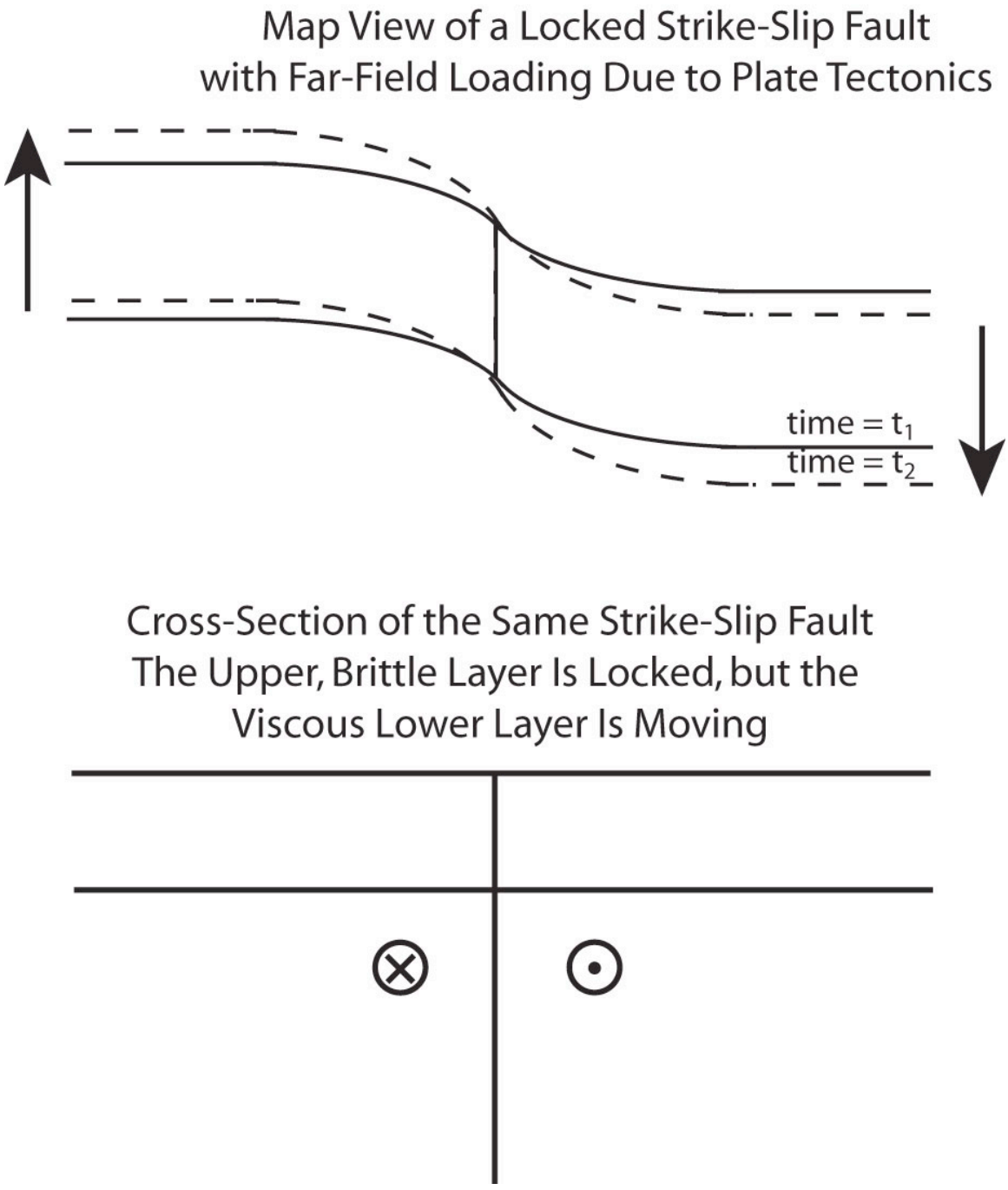

Figure 1.8. *Cartoon of one mechanism that could create our stress rate, $\dot{\sigma}_T$. There is far-field loading of a locked, strike-slip fault that will build up stress in time.*

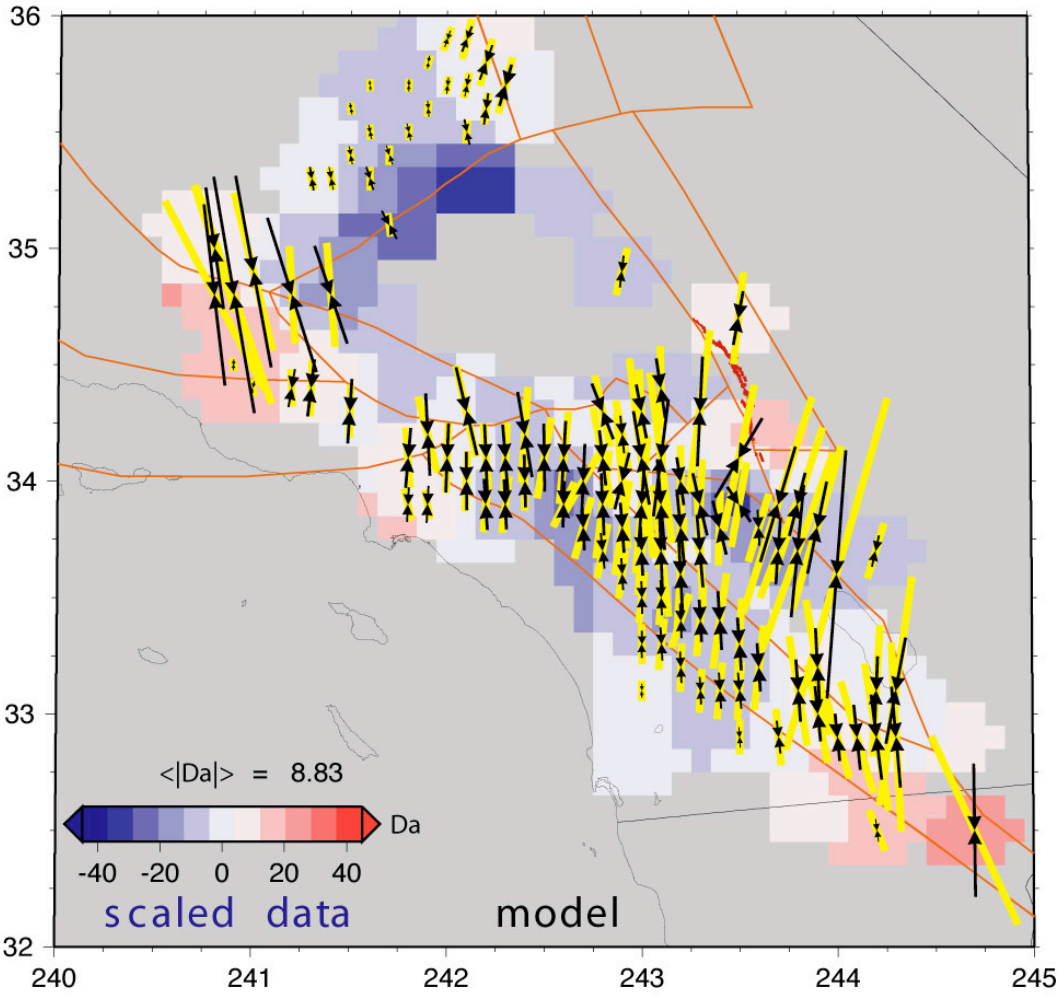

Figure 1.9. *Figure modified from Becker et al. [2003]. They compared the major horizontal compressive axes between: 1) Residual strain rates (in black) modeled from GPS data and block fault models and 2) regional stress inversions (in yellow) from earthquake focal mechanisms. While there is variation in the strain rate data from region to region, one can pick a region like the Los Angeles Basin where there is little to no variation in the orientation of the black strain rate vectors, indicating it is possible to use a spatially uniform stress rate tensor,* $\dot{\boldsymbol{\sigma}}_T$*, for some regional studies. At the very least, this shows that the strain rate orientations, and by implication the stress rate orientations, have much less spatial variability than the stress heterogeneity,* $\boldsymbol{\sigma}'_H(\mathbf{x})$.

Assumptions/Limitations of This Stress Formulation

From the outset it is important to clearly indicate the assumptions used in this thesis and the possible limitations. We do not attempt to create stress heterogeneity in 3D from first principals because of the inherent difficulties. Aagaard and Heaton have numerically created self-sustaining heterogeneous stress on a 2D plane that repeatedly ruptures in time through a dynamic calculation [*Aagaard and Heaton*, personal communication]. However, to faithfully create realistic 3D stress heterogeneity, one would have to numerically simulate all the faults in the region at all lengthscales, from a small 10 cm dislocation to a 100 km rupture, and simulate appropriate spatial distributions of slip for every rupture, throughout thousands of years, because the current stress heterogeneity pattern is a superposition of all the past faulting and fracture history in the crust. Not only does this require many assumptions, such as the distributions of fault orientations, fault lengths, slip on fault, etc., it is also currently numerically impossible using dynamic fracture simulations. Therefore, we have chosen to approach this problem statistically in a simple manner. On the plus side, this enables us to describe spatially heterogeneous stress with two statistical parameters, HR and α, generate synthetic focal mechanisms quickly, and compare our simulations with real data to constrain the statistical properties of the crust. On the other hand, this statistical approach makes many simplifying assumptions in an attempt to obtain a first-cut answer about the statistics of the Earth's crust and overlooks details that are necessary if one wishes to model stress heterogeneity from first principles.

First, while we satisfy rotational equilibrium when we create our stress tensors, we do not satisfy the other equilibrium equation, $\sum_{j=1}^{3} \frac{\partial \sigma_{ij}}{\partial x_j} = f_i$, which specifies no internal accelerations if there are no sources. In order to satisfy $\sum_{j=1}^{3} \frac{\partial \sigma_{ij}}{\partial x_j} = f_i$ and have spatially heterogeneous stress, we would have to include sources, which requires a whole set of additional assumptions; see the beginning of Chapter 3 for a more thorough explanation as to why we do not satisfy the equilibrium equation, $\sum_{j=1}^{3} \frac{\partial \sigma_{ij}}{\partial x_j} = f_i$.

This leads to some of our other assumptions: 1) We do not allow for slip on pre-existing faults. This means our seismicity tends to cluster in 3D clouds rather than lineations or planes as seen in the real Earth. 2) We only allow for point source dislocations. 3) We do not update the stress field after a failure; hence, there is no explicit interaction between events. Equation (1.1) is written for stress inversions of background seismicity where stress perturbations due to individual events are small and should have little to no effect on the other events included in the regional inversions. 4) There is no inclusion of creep, which could change the heterogeneous stress distribution. 5) We assume failure occurs on fresh-fracture, maximally oriented planes at $\pm 45°$ from the σ_1 and σ_3 principal stress axes. This is a consequence of using a plastic yield criterion. In Appendix C, we do use a Coulomb Failure criterion and find similar but more complicated results when we compare our results for Coulomb Failure criterion to our results for the plastic yield criterion in Chapter 4. 6) Last, the spatial stress heterogeneity in the Earth may not vary exactly as a fractal according to our formulation described in Chapters 2 and 3.

A major difference between the assumptions in this thesis vs. those in stress inversions is summarized in Table 1.1. We are assuming an end-member model, heterogeneous stress and homogeneous nucleation strength, whereas stress inversions [*Angelier*, 1975; 1984; *Carey and Brunier*, 1974; *Etchecopar, et al.*, 1981; *Gephart*, 1990; *Gephart and Forsyth*, 1984; *Mercier and Carey-Gailhardis*, 1989; *Michael*, 1984; 1987] represent the other end-member model, homogeneous stress but heterogeneous strength. To understand this difference it is helpful to review some of the basic steps of stress inversions. Figure 1.10, from Angelier [1990], diagrams part of this procedure. One begins by collecting a set of earthquake focal mechanisms in a study region for some time window. The focal mechanisms are converted into slip vectors on a plane that can be described by the parameters strike, dip, and rake, or by a slip vector, $\vec{s}_K$, and normal vector, $\hat{n}_K$, as shown in Figure 1.10 a). An estimated spatially uniform stress tensor, $\boldsymbol{\sigma}_K$, is resolved onto each plane to produce normal traction vectors, $\vec{\sigma}_{N_K}$, and shear traction vectors, $\vec{\tau}_K$, as shown in Figure 1.10 b). The relative angles between the actual slip vectors, $\vec{s}_K$, and the projected shear traction vectors, $\vec{\tau}_K$, are called the misfit angles as shown in Figure 1.10 c). The inversion routine attempts to find a best-fit spatially uniform stress tensor, $\boldsymbol{\sigma}_K$, that minimize the overall misfit statistics. A study by Rivera and Kanamori [2002] of data in Southern California showed that one needs either heterogeneous friction (strength), heterogeneous stress, or both to describe the inversion statistics of real data. Current interpretations of stress inversions assume the stress is spatially homogeneous, and the strength is heterogeneous. In contrast, for our modeling we explain the misfit statistics with heterogeneous stress and assume that the physical processes initiating rupture are homogeneous, i.e., homogeneous nucleation strength.

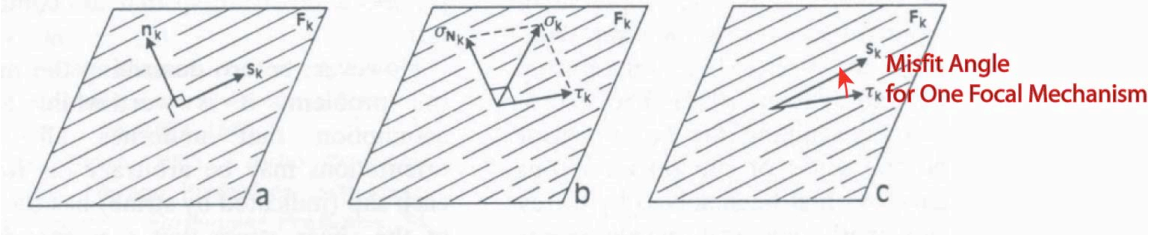

Figure 1.10. *Figure modified from Angelier [1990]. a) The slip plane, slip vector and normal vector to the slip plane for a single focal mechanism. b) Best guess spatially homogeneous stress tensor resolved into normal and shear tractions on the fault plane. c) The relative angle between the shear traction vector for the best guess spatially homogeneous stress tensor and the focal mechanism slip vector. This relative angle is called the misfit angle.*

Table 1.1. Two End Member Models for Explaining the Misfit Statistics of Focal Mechanism Inversions

Current Assumptions in Stress Inversion Modeling	**Assumptions Used in Our Modeling, the Other End-Member Case**
Heterogeneous Nucleation Strength	Homogeneous Nucleation Strength
Homogeneous Stress	Heterogeneous Stress

Overview of Thesis

The method used to generate the heterogeneous stress, $\boldsymbol{\sigma}'_H(\mathbf{x})$, is explained in detail in Chapters 2 and 3. Chapter 2 explains how to generate a scalar quantity with fractal characteristics in 3D. Chapter 3 explains how we generated a full tensorial quantity with fractal characteristics in 3D, i.e., where 5–6 independent quantities have been filtered spatially (5 if one is working with a deviatoric stress tensor, 6 if one is working with a full stress tensor).

In Chapter 4, we describe how we create our synthetic focal mechanism catalogs combining the Hencky-Mises plastic yield criterion with equation (1.1). That chapter explains why stress inversions will be biased towards the orientation of time-varying stress terms, be it the far-field plate tectonic stress rate, $\dot{\boldsymbol{\sigma}}'_T$, or the stress perturbations associated with a mainshock that occurs at time T_E. Appendix C demonstrates numerically that the same bias occurs when one uses the Coulomb Failure Criterion, but the results become more complicated for $\mu \neq 0.0$, because the two conjugate planes are no longer perpendicular. In Chapter 4, we also explore the consequences of the bias towards the stress rate, $\dot{\boldsymbol{\sigma}}'_T$, for the case of background seismicity, in between mainshocks. We find that if stress is highly heterogeneous, the standard stress inversions of focal mechanisms [*Angelier*, 1975; 1984; *Carey and Brunier*, 1974; *Etchecopar, et al.*, 1981; *Gephart*, 1990; *Gephart and Forsyth*, 1984; *Mercier and Carey-Gailhardis*, 1989; *Michael*, 1984; 1987] simply yield $\dot{\boldsymbol{\sigma}}'_T$, instead of $\boldsymbol{\sigma}'_B$, if $\dot{\boldsymbol{\sigma}}'_T$ and $\boldsymbol{\sigma}'_B$ have different orientations. Whereas, if there is little to no heterogeneity, the inversions do yield $\boldsymbol{\sigma}'_B$ as commonly thought.

In Chapter 5, we begin estimating stress heterogeneity parameters, α and HR, in the real Earth. Our estimates for the amplitude of the heterogeneity, HR, is more robust than our estimates for the spatial smoothing, α; however, we find that the increasing bias toward $\dot{\boldsymbol{\sigma}}'_T$ with increasing heterogeneity amplitude, HR, is independent of the α we use for $\alpha \leq 1.0$. Determining the value of α has important implications for calculating the strength of the crust as a function of length-scale, but it does not affect our observations that focal mechanism inversions are biased toward $\dot{\boldsymbol{\sigma}}'_T$ when there is spatially heterogeneous stress. Our best estimate for stress heterogeneity in Southern California, $HR \approx 1.25$, produces stress inversion orientations rotated approximately 30–40% from $\boldsymbol{\sigma}'_B$ toward the stress rate tensor, $\dot{\boldsymbol{\sigma}}'_T$, a non-trivial bias. This result suggests that stress studies using focal mechanism inversion routines [*Angelier*, 1975; 1984; *Carey and Brunier*, 1974; *Etchecopar, et al.*, 1981; *Gephart*, 1990; *Gephart and Forsyth*, 1984; *Mercier and Carey-Gailhardis*, 1989; *Michael*, 1984; 1987] need to be reinterpreted. In light of this, we suggest a new procedure for interpreting focal mechanism inversions where the bias toward $\dot{\boldsymbol{\sigma}}'_T$ would be subtracted out to yield the actual $\boldsymbol{\sigma}'_B$.

References

Aagaard, B., and T. H. Heaton (in preparation, 2006), The influence of prestress, fracture energy, and sliding friction on slip heterogeneity.

Andrews, D. J. (1980), A stochastic fault model: 1) Static case, *Journal of Geophysical Research*, *85*, 3867–3877.

Andrews, D. J. (1981), A stochastic fault model: 2) Time-dependent case, *Journal of Geophysical Research*, *86*, 821–834.

Angelier, J. (1975), Sur l'analyse de mesures recueilles dans des sites faillés: l'utilité d'une confrontation entre les méthodes dynamiques et cinématiques, *C.R. Acadamy of Science, Paris, D*, *283*, 466.

Angelier, J. (1984), Tectonic analysis of fault slip data sets, *Journal of Geophysical Research*, *89*, 5835–5848.

Angelier, J. (1990), Inversion of field data in fault tectonics to obtain the regional stress .3. A new rapid direct inversion method by analytical means, *Geophyiscal Journal International*, *103*, 363–376.

Barnsely, M., et al. (1988), *The Science of Fractal Images*, Springer-Verlag, New York.
Barton, C. A., and M. D. Zoback (1994), Stress perturbations associated with active faults penetrated by boreholes: Possible evidence for near-complete stress drop and a new technique for stress magnitude measurement, *Journal of Geophysical Research*, *99*, 9373–9390.

Becker, T. W., et al. (2003), Constraints on the mechanics of the Southern San Andreas fault system from velocity and stress observations, paper presented at 2003 SCEC Annual Meeting, Southern California Earthquake Center, Oxnard, California, September 7–11, 2003.

Ben-Zion, Y., and C. G. Sammis (2003), Characterization of fault zones, *Pure and Applied Geophysics*, *160*, 677–715.

Carey, E., and B. Brunier (1974), Analyse théorique et numérique d'un modèle méchanique élémentaire appliqué à l'étude d'une population de failles, *C.R. Acadamy of Science, Paris, D*, *279*, 891–894.

Dieterich, J. H. (2005), Role of stress relaxation in slip of geometrically complex faults, paper presented at American Geophysical Union, San Francisco, December 2005.

Etchecopar, A., et al. (1981), An inverse problem in microtectonics for the determination of stress tensors from fault striation analysis, *Journal of Structrual Geology*, *3*, 51–65.

Gephart, J. W. (1990), FMSI: A Fortran program for inverting fault/slickenside and earthquake focal mechanism data to obtain the regional stress tensor, *Computers and Geosciences*, *16*, 953–989.

Gephart, J. W., and D. W. Forsyth (1984), An improved method for deteremining the regional stress tensor using earthquake focal mechanism data: Application to the San Fernando earthquake sequence, *Journal of Geophysical Research*, *89*, 9305–9320.

Herrero, A., and P. Bernard (1994), A kinematic self-similar rupture process for earthquakes, *Bulletin of the Seismological Society of America*, *84*, 1216–1228.

Lachenbruch, A. H., and J. H. Sass (1980), Heat-flow and energetics of the San-Andreas fault zone, *Journal of Geophysical Research*, *85*, 6185–6222.

Lavallee, D., and R. J. Archuleta (2003), Stochastic modeling of slip spatial complexities of the 1979 Imperial Valley, California, earthquake, *Geophysical Research Letters*, *30*, Art. No. 1245.

Liu-Zeng, J., et al. (2005), The effect of slip variability on earthquake slip-length scaling, *Geophysical Journal International*, *162*, 841–849.

Mai, P. M., and G. C. Beroza (2002), A spatial random field model to characterize complexity in earthquake slip, *Journal of Geophysical Research-Solid Earth*, *107*, Art. No. 2308.

Manighetti, I., et al. (2005), Evidence for self-similar, triangular slip distributions on earthquakes: Implications for earthquake and fault mechanics, *Journal of Geophysical Research-Solid Earth*, *110*, Art. No. B05302.

Manighetti, I., et al. (2001), Slip accumulation and lateral propagation of active normal faults in Afar, *Journal of Geophysical Research*, *106*, 13667–13696.

McGill, S. F., and C. M. Rubin (1999), Surficial slip distribution on the central Emerson fault during the June 28, 1992 Landers earthquake, California, *Journal of Geophysical Research-Solid Earth*, *104*, 4811–4833.

Mercier, J.-L., and S. Carey-Gailhardis (1989), Regional state of stress and characteristic fault kinematics instabilities shown by aftershock sequence: the aftershock sequence of the 1978 Thessaloniki (Greece) and 1980 Campania-Lucania (Italy) earthquakes as examples, *Earth and Planetary Science Letters*, *92*, 247–264.

Michael, A. J. (1984), Determination of stress from slip data: Faults and folds, *Journal of Geophysical Research-Solid Earth*, *89*, 11517–11526.

Michael, A. J. (1987), Use of focal mechanisms to determine stress: A control study, *Journal of Geophysical Research-Solid Earth*, *92*, 357–368.

Rice, J. R. (1999), Flash heating at asperity contacts and rate-dependent friction, paper presented at American Geophysical Union, San Francisco.

Rice, J. R., et al. (2001), Rate and state dependent friction and the stability of sliding between elastically deformable solids, *Journal of the Mechanics and Physics of Solids*, *49*, 1865–1898.

Rivera, L., and H. Kanamori (2002), Spatial heterogeneity of tectonic stress and friction in the crust, *Geophysical Research Letters*, *29*, art. no. 1088.

Sibson, R. H. (2003), Thickness of the seismic slip zone, *Bulletin of the Seismological Society of America*, *93*, 1169–1178.

Townend, J., and M. D. Zoback (2004), Regional tectonic stress near the San Andreas fault in central and southern California, *Geophysical Research Letters*, *31*, 1–5.

Tullis, T. (2005), Dramatic reductions in fault friction at earthquake slip rates, edited. Tullis, T. E., and D. L. Goldsby (2005), paper presented at Chapman Conference on Radiated Energy and the Physics of Earthquake Faulting, Portland, Maine, June 13–17, 2005.

Wald, D. J., and T. H. Heaton (1994), Spatial and temporal distribution of slip for the 1992 Landers, California, earthquake, *Bulletin of the Seismological Society of America*, *84*, 668–691.

Wilde, M., and J. Stock (1997), Compression directions in southern California (from Santa Barbara to Los Angeles Basin) obtained from borehole breakouts, *Journal of Geophysical Research*, *102*, 4969–4983.

Zoback, M. D., and G. C. Beroza (1993), Evidence for near-frictionless faulting in the 1989 (M 6.9) Loma Prieta, California, earthquake and its aftershocks, *Geology*, *21*, 181–185.